NASA Technical Memorandum 102409

Real-Time Simulation of an F110/STOVL Turbofan Engine

Colin K. Drummond and Peter J. Ouzts
Lewis Research Center
Cleveland, Ohio

Prepared for the
Central/Northeastern ADIUS Conference
sponsored by Applied Dynamics International
Cleveland, Ohio, October 16-17, 1989

NASA

REAL-TIME SIMULATION OF AN F110/STOVL TURBOFAN ENGINE

Colin K. Drummond and Peter J. Ouzts

National Aeronautics and Space Administration
Lewis Research Center
Cleveland, Ohio 44135

ABSTRACT

A traditional F110-type turbofan engine model has been extended to include a ventral nozzle and two thrust-augmenting ejectors for Short Take-Off Vertical Landing (STOVL) aircraft applications. Development of the real-time F110/STOVL simulation required special attention to the modeling approach to component performance maps, the low pressure turbine exit mixing region, and the tailpipe dynamic approximation. Simulation validation derives by comparing output from the ADSIM simulation with the output for a validated F110/STOVL General Electric Aircraft Engines FORTRAN deck. General Electric substantiated basic engine component characteristics through factory testing and full scale ejector data.

INTRODUCTION

An Integrated Controls Research Demonstrator program is underway with the objective of developing and validating technology for integrated-flight propulsion control design methodologies for Short Take-Off Vertical Landing (STOVL) aircraft. This research effort is part of the NASA STOVL technology program to provide the propulsion technologies which must be in place to permit a low-risk decision regarding the initiation of a supersonic technology demonstrator aircraft in the mid-1990's.

The proposed E-7D aircraft is based on an F-16 airframe and a F110-type engine (see Jenista et.al. [1987]). STOVL capabilities derive from the installation of two ejector augmentors, a ventral nozzle, a reaction control system (RCS), and a 2D-CD cruise nozzle; these devices can be thought of as propulsion control effectors. Conventional elevons and rudders serve as aerodynamic control effectors. Approximate component locations on the E-7D are shown in Fig. 1. Manual control effector integration for this aircraft is expected to be a difficult, high pilot workload situation for three basic reasons: (1) the *number* of control effectors, (2) the coupled nature of the airframe/propulsion controls, and (3) the additional airframe/propulsion interactions. Low speed flight creates an especially complex pilot integration task since propulsion and aerodynamic control devices are used simultaneously. For these reasons, it is clear the E-7D aircraft must incorporate an integrated flight/propulsion control system (IFPC).

The Integrated Controls Research Demonstrator program is depicted in Figure 2. Propulsion system hardware (including the control) will be mounted on the NASA-Lewis Powered Lift Facility (PLF). The aircraft and its flight dynamics along with a simulation of a human pilot will be simulated. An integrated control (propulsion system and flight control) will be programmed into a real flight-type breadboard control computer. System evaluation will be accomplished by using a paper pilot to "fly" the aircraft through prescribed flight exercises. Testing at this point will also include further ejector dynamics validation and reaction control bleed effects on the engine. Subsequent to this experimental program, a final phase of evaluation will include ground effects testing of the E-7D on the NASA-Ames Outdoor Aerodynamic

Research Facility (OARF), large-scale aerodynamics testing on the National Full-Scale Aerodynamics Complex (NFAC) at NASA-Ames, and final integrated control evaluation for handling qualities on the NASA-Ames Vertical Motion Simulation (VMS).

An essential element of the integrated control design effort is a realtime-simulation of the propulsion system -- it is useful in control concept design, evaluation, and testing. The present work describes a realtime digital simulation of an F110-type engine configured for STOVL aircraft applications; a high-speed multi-processor digital computer, designated the AD100, is used for the code execution since the AD100 is specifically designed for high-speed simulation of continuous dynamic systems.

Propulsion System Simulation Perspective

The E-7D simulation overview shown in Figure 3 emphasizes two general features the final E-7D simulation will offer: one is the pilot interface options and the other is the engine hardware drop-in capability. The "paper pilot" refers to the work of Vogt et. al. [1989] at the University of Pittsburgh which has resulted in a computer simulation of a pilot in V/STOL aircraft. Although a man-in-the-loop simulation capability is planned as an alternative to the Pittsburgh paper pilot, it is expected the paper pilot will initially provide the necessary input to the Maneuver Command Generator (MCG).

The second feature the final system will provide is the selection between F110-type hardware and the real-time simulation. For preliminary E-7D simulation operation, the ADSIM F110/STOVL simulation will mimic the engine plant and the propulsion control operation. For the PLF tests the hardware option will be invoked. It is anticipated that the transition from software to hardware will require some fine tuning of the control; in that event a modular simulation approach simplifies the ensuing iterations between software and hardware. It is evident that the various propulsion module and pilot interface options require a flexible simulation structure and clearly defined module interfaces.

Two System 100 computers will ultimately be involved in the NASA-Lewis PLF simulation, one for the propulsion system simulation and another for the airframe simulation; the two systems interact through real-time input/output commands (ADRIO). The arrangement of the AD100 computers and communication paths is depicted in Fig.4. Although this may appear to initially complicate the overall E-7D system simulation, such a configuration permits the engine software to be rapidly replaced with engine hardware. The NASA-Ames VMS tests will combine the engine and airframe simulation on one AD100 unit.

With a general IFPC schematic in mind, a complete propulsion system in the present work is perceived as the sum of four basic sub-systems. Figure 5 illustrates the F110/STOVL engine module must be joined by control, actuator, and sensor modules in order to form a propulsion *system*. Current research focuses primarily on the engine module. Parallel research is in-progress on control design methodologies for STOVL aircraft. This paper describes the current results from the recent engine modeling effort; the F110/STOVL control development in-progress is an application of modern multivariable control theory (see, for example Akhter et. al.[1989]).

F110/STOVL Engine Model

A highly detailed turbofan engine simulation is required for accurate propulsion system representation. A useful and practical real-time simulation approach involves tieing together several basic engine components. Fig. 6 depicts a proposed STOVL-configured turbofan engine component assembly and associated system control variables. Each component's mathematical description is obtained by applying basic conservation laws that focus on the physics of interest.

This general approach has been previously implemented on hybrid computers (see Szuch et. al.[1982] and Seldner et. al.[1972]) and more recently on digital computers (ADI[1987], Ballin[1988]).

Of specific interest in the F110/STOVL simulation are the propulsion system components unique to STOVL aircraft, particularly thrust augmenting ejectors, feeder pipes, and a ventral nozzle. Also of interest is the effect that, for instance, the presence of the ejector and ventral nozzle will have on tailpipe dynamics. In order to capture the basic propulsion system simulation philosophy in the present work, two aspects of the simulation that have the most impact on simulation speed, accuracy, and coding are discussed. First, the general framework of the gas generator portion of the F110/STOVL engine is discussed, with specific emphasis on the component map characteristics and the component coupling technique. Second, modelling approaches required to accommodate the mixing, stratification, and volume dynamics of the STOVL facet of the engine are summarized.

Gas Generator

The F110/STOVL turbofan engine gas generator model is composed of compressor (low and high pressure) models, a burner model, turbine (high and low pressure) models, and associated gas flowpath models linking each major component. The gas generator model predicts gas flowpath properties up to the mixing plane of the high pressure and low pressure (bypass) gas flows. The STOVL specific volume dynamics routines (discussed later in this paper) perform the subsequent gas flowpath mixing and routing to the various STOVL thrust producing nozzles. The formulation of the F110/STOVL gas generator model for use on the AD100 primarily involved translation of a F110/STOVL FORTRAN engine model to ADSIM syntax and conventions. However, two modeling techniques inherent in the base F110/STOVL FORTRAN model which were retained in the AD100 version warrant discussion.

Component Performance Representations

A major task in turbofan engine modeling is predicting the aerothermal performance of the major components of the engine. The traditional approach to the modeling of turbofan component performance has been based on non-dimensional analysis. This approach yields multivariate component "maps" which detail base component performance over a wide range of operating conditions. An example of such a nondimensional performance map for a generic fan block (Fig. 7a) is the low pressure compressor (fan) map shown on Fig. 7b. A similar approach yields performance maps to predict performance of the remaining rotating components of the engine.

The non-dimensional performance map is a relatively straight forward and an intuitively pleasing approach to turbofan component performance modeling. However, as a practical modeling technique, the approach has some significant drawbacks. Traditional component maps are not easily scaled; therefore the maps are limited in their use for modification of component performance to account for new data and/or component sizing studies. Furthermore, modeling of component off-design performance can require additional maps consuming large amounts of computer memory.

The drawbacks in the traditional turbofan component performance maps led to the development of alternative methods of modeling component performance. Converse and Griffin[1984] present a "backbone" performance fitting technique based on the physics of the component rather than curvefits of nondimensional parameters. The basic computational module for the backbone performance specification is summarized in Fig. 7c. A key to the approach is the specification of a work coefficient delta from the component backbone operating condition

which thereby sets the performance of the component. An example of a work coefficient delta would be, for instance, the difference between the actual and minimum-loss (i.e. backbone) work coefficents for a fan

$$\Delta\psi = \psi - \psi_{ML}$$

where the work coefficient ψ can be given by the non-dimensional enthalpy rise across the fan

$$\psi = \frac{\Delta h_2}{c_p T_{ref}}$$

Backbone maps have the advantage of being easily scaled to account for component variations as described above. The backbone performance map technique was utilized for rotating component performance modeling in the base FORTRAN F110/STOVL model and was retained in the AD100 version.

Intercomponent Coupling

Corollary to the task of predicting individual component performance is the matching of component operating conditions such that basic conservation laws are obeyed along the gas flowpath. One approach to this problem is to explicitly invoke conservation laws in the form of differential equations relating the flowpath conditions between major components. This approach has been implemented on previous AD100 turbofan simulations (see ADI[1987]) and was first envisioned for the F110/STOVL AD100 model. A block diagram depicting the intercomponent volume dynamic routines was shown previously in Fig. 6.

An alternative technique of matching component operating conditions is to employ performance "states" which (directly and indirectly) set the operating conditions of the major components of the gas generator model. An example of a performance state is the work coefficient delta used to specify compressor operating condition using the backbone performance map technique described above. Performance states are generated by the introduction of error "states". Error states primarily relate to continuity between rotating turbofan components. An example of an error state is the difference between gas flow energy output from the burner and gas flow energy input required by the high pressure turbine to drive the core compressor. The error states are multiplied by a gain matrix to compute the next set of performance states to set component operating conditions.

$$\begin{Bmatrix} \text{Perf} \\ \text{States} \end{Bmatrix} = \begin{bmatrix} \text{Gain} \\ \text{Matrix} \end{bmatrix} \begin{Bmatrix} \text{Error} \\ \text{States} \end{Bmatrix}$$

The performance and error state loop acts as a feedback mechanism to match individual component performance. Ideally, this feedback loop is exercised until error states are below a specified tolerance. The gas generator then operates in a quasi-steady state mode with only rotor and gas-metal heat transfer dynamics present. However, to save computational time only a single pass through the loop is executed. Only during large transients do the error states become significantly large as to preclude the quasi-steady state mode and normally the errors return to small magnitude after several time steps. A block diagram of a typical implementation of performance and error state for a turbofan engine gas generator model is shown on Fig. 8.

The F110/STOVL FORTRAN model used as the base for the AD100 model utilizes the performance and error state technique for matching component performance. This technique was retained in the AD100 version for two reasons. First, several performance states used in the backbone component performance map representation are generated by the performance and error state loop. Although the required backbone map inputs could be generated from intercomponent volume dynamic results, such a correlation would have to be developed. A simpler approach would be to obtain component performance data in the traditional nondimensional component map form, however this data was not readily available.

The second and more important reason for retaining the performance and error state formulation involves the basic requirements of the modeling task. The F110/STOVL model developed here is for use in an integrated flight and propulsion simulation. The projected integration time step for this simulation is on the order of 10 msec (the airframe simulation may operate at even larger time steps). The required gas generator model is then low frequency when compared to the intercomponent volume dynamics present in the gas generator (this is not the case for the gas flowpath mixing regions; hence later discussions on mixing region volume dynamics). Only rotor and gas-metal heat transfer dynamics are of consequence at this low frequency, therefore the quasi steady-state mode present in the performance and error state formulation are adequate for the simulation task.

While inclusion of an explicit intercomponent volume dynamics equations would result in a higher frequency (and possibly higher fidelity) gas generator model, such a model is not required by the simulation task. Furthermore, a high frequency model may result in dynamic instabilities requiring additional computational burden (i.e., smaller time steps) or appropriate dynamic damping to resolve. Therefore, the use of the performance and error state technique for the gas generator portion of the F110/STOVL model ideally suited the simulation task.

STOVL Component Approximation

Analysis of the proposed E-7D configuration has provided an opportunity to investigate multi-stream mixing and the dynamics of components with potentially significant volume dynamics effects. Although the frequency content of previous turbofan engine simulations provided some technical antecedent for the quasi-steady volume dynamic approximation in the gas generator portion of the engine, such an assumption is difficult to make a priori for the "back-end" of the engine. A sketch of the proposed locations for the ventral nozzle, ejectors, and aft nozzle was shown in Figure 1. Figure 9 illustrates the interpretation of this configuration in terms of a component level model. Distinctions are made between mixing plane dynamics, main nozzle stratification, and the main nozzle, ventral nozzle, and ejector force effectors. Determining the "best" models to use involved the usual analytic challenge of constructing the most detailed component representation whose solution is amicable to real-time simulation. Specific remarks on modeling techniques and assumptions for each model in the proposed STOVL configuration follow. For brevity, comments on generic nozzle behavior are not made here since extensive analyses can be found elsewhere (see, for instance Cohen et. al. [1987])

Mixing Region Dynamics

Representation of the fan-bypass stream and low pressure turbine (LPT) discharge stream confluence requires analysis of (a) two-stream mixing and (b) local volume dynamics; the combined problem is approximated in what will be termed the mixing region dynamics block. Control-volume approaches to multi-stream mixing provide an excellent foundation for real-time simulations; an example for steady flow is given in the work of Mattingly et. al.[1986], while

Szuch et. al.[1982] present an approach for transient flow analysis. The present work combines a generalized form of the pressure derivative from the heat equation (see the analysis of Drummond[1989] or Szuch[1982])

$$\frac{dP_k}{dt} = \frac{\gamma - 1}{V_k}\{\sum m_i h_i - \sum m_j h_k\}$$

with the time derivative form of the state equation

$$\frac{dh_k}{dt} = \frac{h_k}{P_k V_k}(\gamma - 1)\left\{(\sum \dot{m}_i h_i - \sum \dot{m}_j h_j) - \frac{h_k}{\gamma}\left(\frac{dm}{dt}\right)_k\right\}$$

where the mass accumulation has the usual form

$$\left(\frac{dm}{dt}\right)_k = \sum \dot{m}_i - \sum \dot{m}_j$$

A feature of the analysis is that although the mixing region mass time derivative is required for the enthalpy and pressure derivative computations, the mass efflux from the region is *not* computed by integration of the mass derivative itself. Discharge flow from the mixing region is dictated by feeding back actual demands of the main, ventral, and ejector nozzles. This *system* approach to the mixing region description differentiates it from traditional mixing region analysis.

It is not assumed the specific heat ratio is constant; however, for simplicity, the temperature dependence of γ is given by a polynomial. Gas temperature as a function of enthalpy also has a polynomial form, derived by combining the definition of specific heat

$$c_p = \frac{dh}{dt}$$

with a polynomial approximation for the variation of specific heat with temperature, and then integrating the result (see, for instance, Faires[1946] or Keenan and Kayes [1966] for more details).

Stratification Logic

A traditional turbofan requires the tailpipe mixed flow to feed a single component -- the aft nozzle. However, in the proposed STOVL configuration, the flow requirements of the ventral nozzle and ejectors must also be considered. The detailed fluiddynamic stratification to the STOVL components is an unfortunately complex three-dimensional flow problem whose state-of-the-art solution is not amicable to real-time solution. We elect to trivialize this problem by first recognizing that the STOVL components can be viewed quite simply as a set of nozzles placed strategically about the aircraft. Since generic nozzle performance is primarily a function of nozzle pressure ratio and area ratio, the task of stratification translates into prescription of the total temperature and pressure that feeds each nozzle. Until there appears evidence that specific component behavior biases the tailpipe flow in some other quantifiable way, the stratification logic in the present work is to assume that total pressure and temperature will

respond instantaneously to flow disturbances in a *uniform* manner. That is, the total pressure and temperature feeding each nozzle will be equal; note that we are *not* a priori specifying the *flowrate* to each nozzle for performance calculations.

It is necessary to remark that, for the limited purpose of computing afterburner pressure drop, an estimate of the flowrate to the afterburner must be made. This is possible at any time by subtracting from the mixing region discharge flowrate the demands of the ventral and ejector nozzles computed at the previous timestep.

Also, the stratification block accounts for the influence temperature has on the "new" fuel-to-air ratio (as a result of the bypass stream and LPT discharge mixing).

Thrust Augmenting Ejector

In the proposed E-7D design, thrust augmenting ejectors placed at the root of each wing primarily provide vertical and longitudinal thrust for the aircraft. It has been determined that the dynamic response of the proposed ejectors is so rapid (natural frequency on the order of 300Hz, Drummond[1988]), that a quasi-steady flow approximation is appropriate for typical E-7D operations.

It is necessary to recognize the importance of the quasi-steady flow approximation. In such a situation we are permitted to characterize ejector behavior with steady-state ejector performance maps to describe ejector behavior in the transient engine simulation. The alternative is to include a full dynamic description of the ejector. Given that ejectors are driven by a turbulent shear-layer between the primary and secondary flows, the necessary modeling approach would be to include some form of the Navier-Stokes equations for turbulent flow in the analysis; in such a case the computations are not likely to result in a real-time engine simulation. Future research on ejector simulations is necessary if the desired fidelity of the aircraft simulation approaches the estimated 300Hz ejector threshold.

Due to the prescribed operating range of the E-7D ejectors, only a portion of the generalized ejector performance map shown in Figure 10 is employed in the present simulation. Data for the ejector performance was obtained through full-scale ejector tests conducted in June 1987 at the NASA-Lewis Powered Lift Facility.

Ventral Nozzle

The ventral nozzle, so-named by its location on the underside if the airframe, provides vertical lift to the aircraft, but also a significant measure of pitch control during the powered-lift phase of aircraft flight. A convergent nozzle design was selected for the ventral since it is anticipated to generally encounter subsonic flows. Ventral nozzle performance is therefore given by a scaled performance map of a traditional convergent nozzle of similar area ratio.

CASE STUDY

Two important features the engine simulation must exhibit are accuracy and the capability to be executed faster than real-time. In order to test simulation accuracy, a case is required that will exercise the dynamic features of each component and indicate some response to control variable variation. For the present work it is the addition of STOVL-specific components that is new to the basic engine simulation, so the desired test case should involve all STOVL component operating simultaneously. Rapid changes in STOVL thrust producing components are of interest since strong forcing functions tend to test the accuracy and 'robustness' of the dynamic system more than perturbation inputs do.

Overview of Test Case

A single test case is considered in which a change in fuel flowrate is combined with STOVL component operations. This case is not intended to mimic any specific E-7D flight mode or scenario; conditions are summarized below:

Fuel Flow:

Increase main combustor demand by 3200 pph between $t=1$ and $t=3$ seconds.

Aft Nozzle Area:

Slowly close down the aft nozzle area during the period $t=1$ and $t=4$ seconds, then rapidly close the nozzle to 20 in^2 in the next 2 seconds.

Ventral Nozzle Area:

Initially closed. Start opening at $t=4$ sec and reach 55% open at $t=5$ seconds; continue to open between $t=5$ and $t=6$ to a final value of 73%.

Thrust Augmenting Ejector Flow:

Operate port and starboard ejectors simultaneously and equally. Ejector flowrates controlled by a butterfly valve whose closed position corresponds with a valve angle of 0^o, and whose full open position corresponds with a valve angle of 90 degrees.

The primary objective is to match the dynamic response of the real-time ADSIM engine with the FORTRAN baseline model. Matching steady-state performance is desired, but secondary, in the present simulation.

Discussion of Results

The ADSIM simulation of the F110/STOVL engine was executed on the Applied Dynamics International AD100 processor; a simulation timestep of 10ms combined with the 0.41ms frametime indicates the engine simulation runs approximately 40 times faster than real time. This is encouraging for the ultimate real-time simulation of the E-7D since the E-7D simulation will only run in realtime if all of its subsystems can be executed much faster than real-time.

Comparison of engine rotor speeds is a conventional way to measure simulation accuracy. Figure 11 shows the fan and core speeds of the ADSIM and baseline simulation engines plotted as a function of time. Generally, rotor speeds predicted by ADSIM for steady-state operation are within 2% of the baseline predictions. During dynamic operation the error is within 4%, except for the predictions after $t=6$ sec. There is some question about the baseline model accuracy for ventral nozzle performance between $t=6$ and $t=7$, so comparisons of performance during that period are not appropriate at this time.

Trends for normalized thrust shown in Figure 12 are very encouraging. Both simulations show the expected increase in aft nozzle thrust resulting from the increase in fuel flow. Although the aft nozzle area is closing down during this period, the decrease in thrust (for *only* a nozzle area change) is overpowered by the speedup of the engine associated with the new fuel level the combustor enjoys. A nearly constant 0.6% thrust difference for the simulations between $t=0$ and $t=4$ parallels a similar difference in fan speed. Since it is intended the normalization amplify simulation differences, the fact that the simulations mimic changes in thrust so well remarks

favorably on the dynamic accuracy of the ADSIM simulation. Ejector trends are also very good. As mentioned earlier, the departure in ventral nozzle thrust predictions is of concern beyond the t=6 sec point. Since the sudden change in ventral nozzle thrust in the t=6 sec vicinity for the baseline simulation (indicated by a dashed line) does not intuitively follow the prescribed ventral nozzle area change, a close look at the baseline simulation code is in-progress.

CONCLUDING REMARKS

Some departures in predicted thrust and speed between the ADSIM and baseline engine codes do not significantly erode the general success of the ADSIM code in mimicking the dynamic behavior of the baseline engine code. This permits concluding the following:

1. The baseline FORTRAN F110/STOVL 'backbone'component maps and intercomponent coupling method for the gas generator has been sucessfully invoked in the ADSIM simulation environment, and

2. The renovated mixing region dynamics and stratification logic is an appropriate modeling technique for STOVL configurations.

REFERENCES

1. Akhter,M.M, J.H.Vincent, D.F.Berg, and D.S.Bodden (1989), "Simulation Development for US/Canada ASTOVL Controls Technology Program," 20th Modeling and Simulation Conference, May 4-5, Pittsburgh, Pennsylvania.
2. Applied Dynamics International (1987), "Simulation of a High by-pass Two Spool Engine," System 100 Application Code.
3. Ballin, M. (1988), "A High-Fidelity Real-Time Simulation of a Small Turboshaft Engine," *NASA TM-100991.*
4. Cohen,H., G.F.C.Rodgers, and H.I.H.Saravanamuttoo (1987), *Gas Turbine Theory*, 3rd ed., Wiley and Sons.
5. Converse and Griffin (1984), "Extended Parametric Representation of Compressor Fans and Turbines," *NASA CR-174645.*
6. Drummond, C.K. (1988), "A Control-Volume Method for Analysis of Unsteady Thrust Augmenting Ejector Flows," *NASA CR-182203.*
7. Drummond, C.K. (1989), "STOVL Propulsion System Volume Dynamics Approximations," American Society of Mechanical Engineers, Winter Annual Meeting.
8. Faires, V.M. (1947), *Applied Thermodynamics*, MacMillan Press.
9. Jenista,J.E., and A.E.Sheridan (1987), "Configuration E7 Supersonic STOVL Fighter/Attack Technology Program," SAE Paper 872379.
10. Keenen and Kayes (1966), *Gas Tables*, McGraw-Hill.
11. Mattingly, J.D., W.H.Heiser, and D.H.Daley (1986), *Aircraft Engine Design*, AIAA.
12. Seldner, M., J.Mihaloew, and R.J.Blaha (1972), "Generalized Simulation Technique for Turbojet Engine System Analysis," *NASA TN-D-6610.*
13. Shaw, P. D. (1988), "Design Methods for Integrated Control Systems," AFWAL TR-88-2601.

14. Szuch,J., S.M.Krosel, and W.M.Bruton (1982), "Automated Procedure for Developing Hybrid Computer Simulation of Turbofan Engine," *NASA TP-1851.*

15. Vogt, W.G., M.H.Mickle, M.E.Zipf, and S.Kucuk (1989), "Computer Simulation of a Pilot in V/STOL Aircraft Control Loops," Final Report for NASA Grant NAG-3-729.

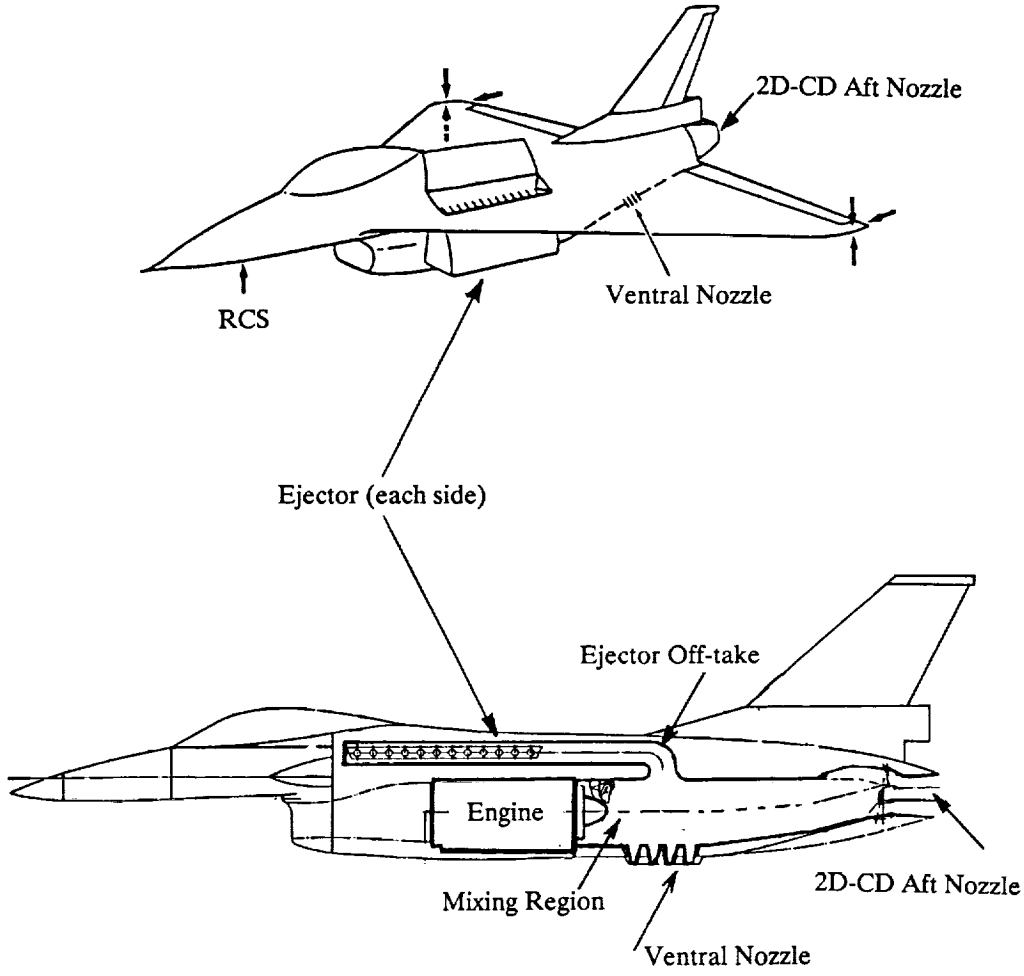

Fig. 1 E-7D/Ejector configured aircraft.

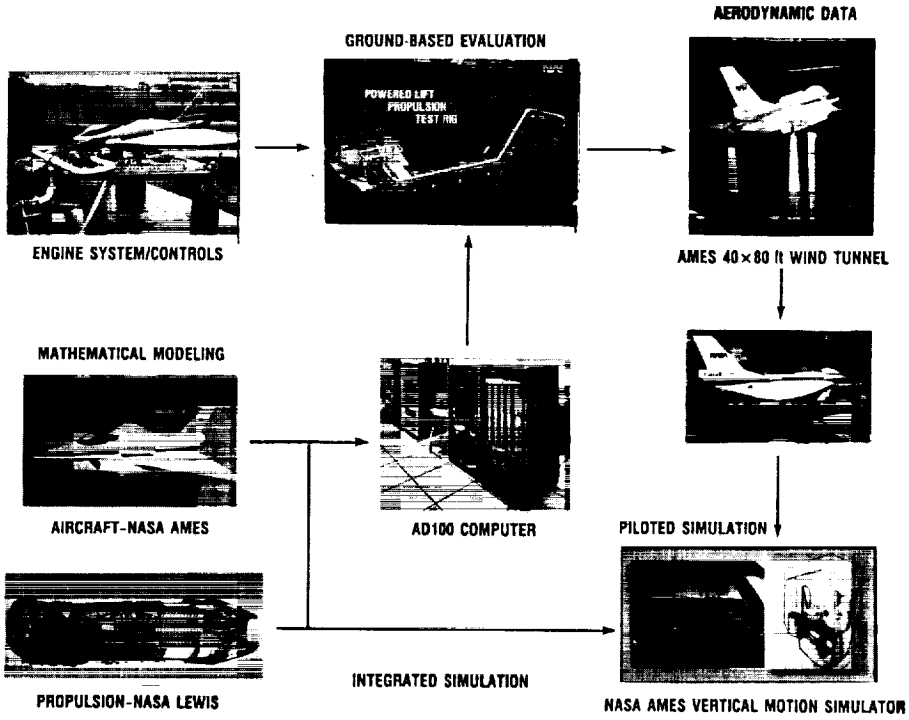

Fig. 2 Integrated controls research demonstrator program.

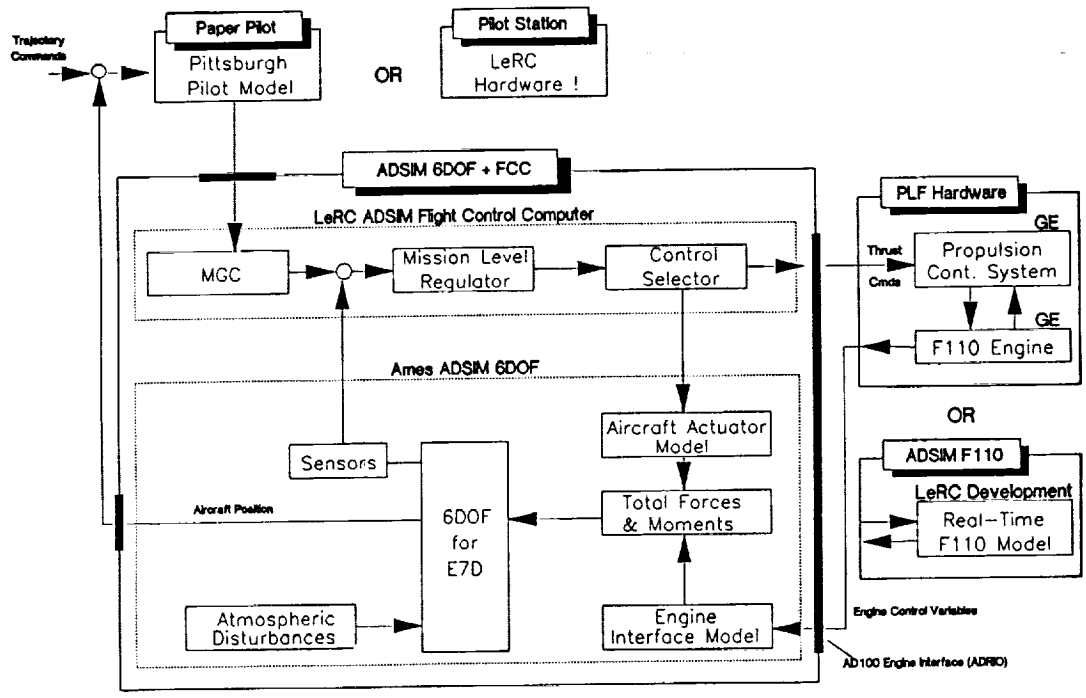

Fig. 3 Overview of E-7D simulation structure and options.

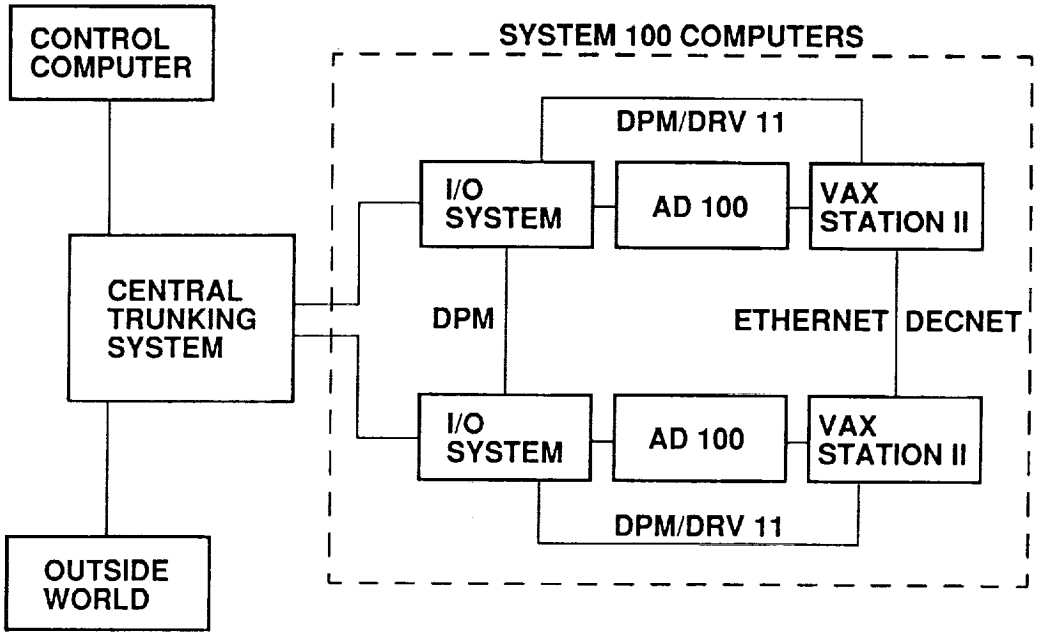

Fig. 4 System 100 digital simulation computers and communication paths.

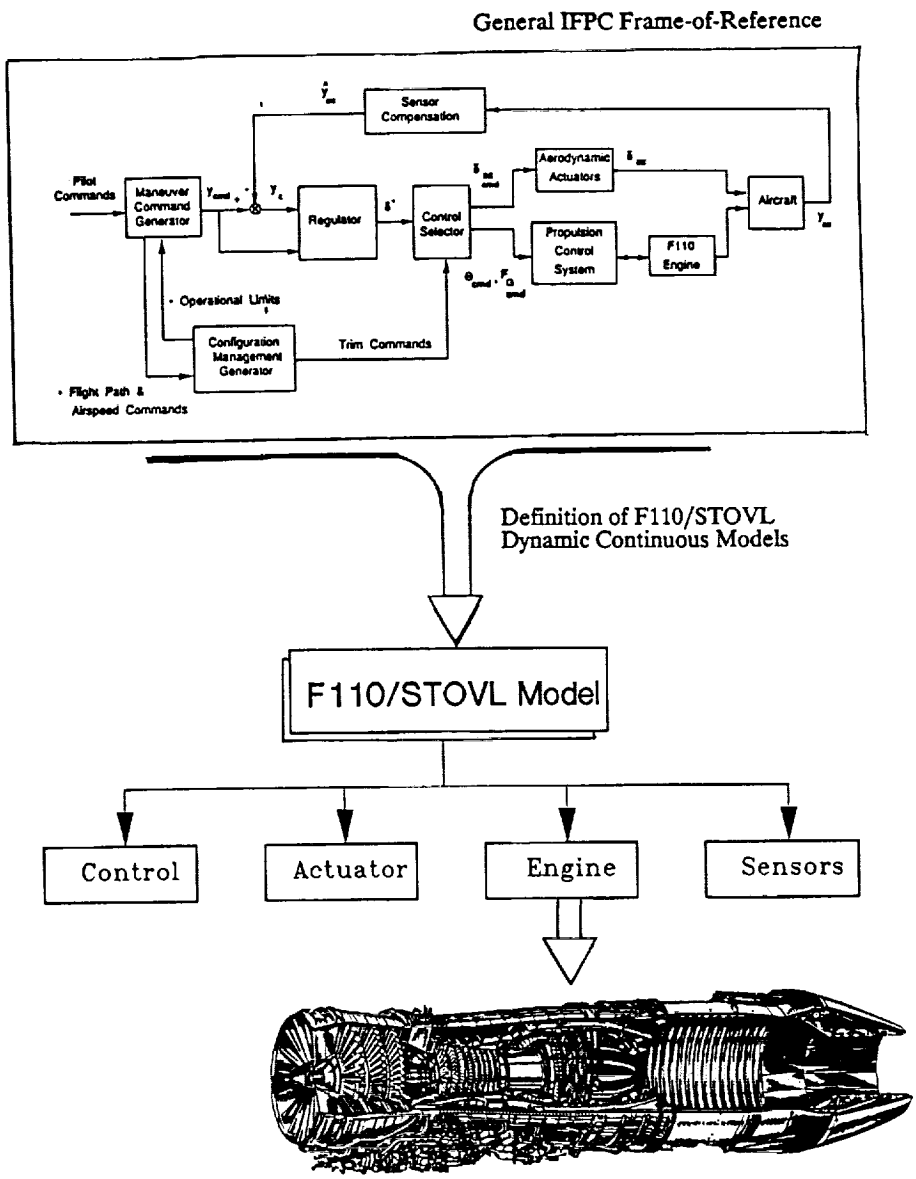

Approximate Engine by a Component Level Model

Fig. 5 General F110/STOVL ADSIM Modules

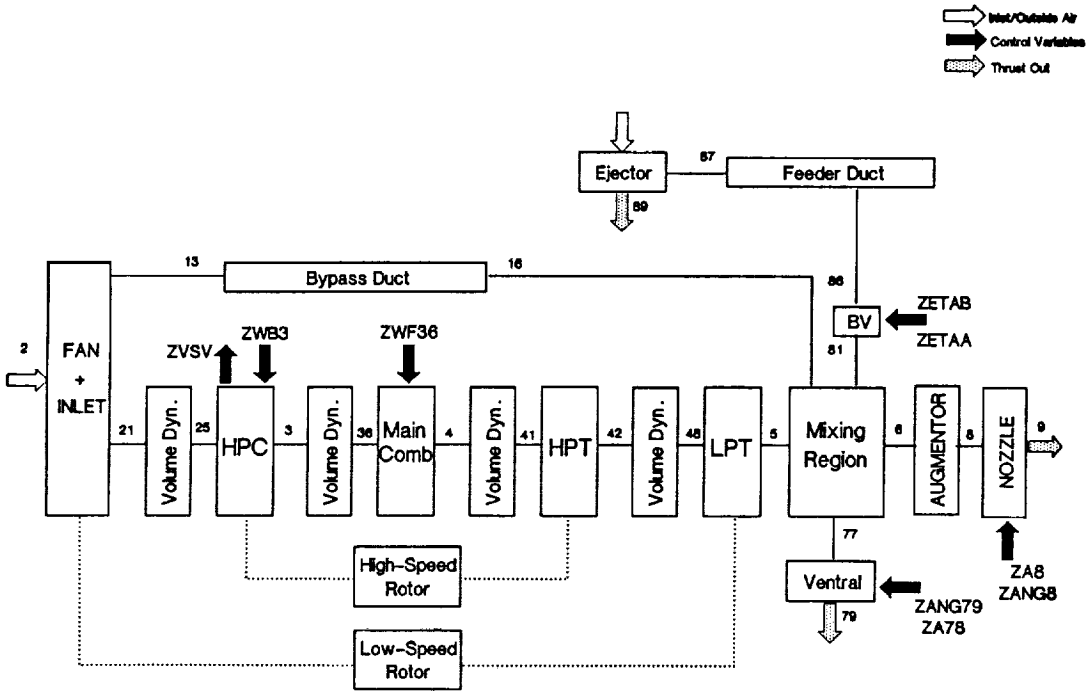

Fig. 6 Baseline propulsion system component level model.

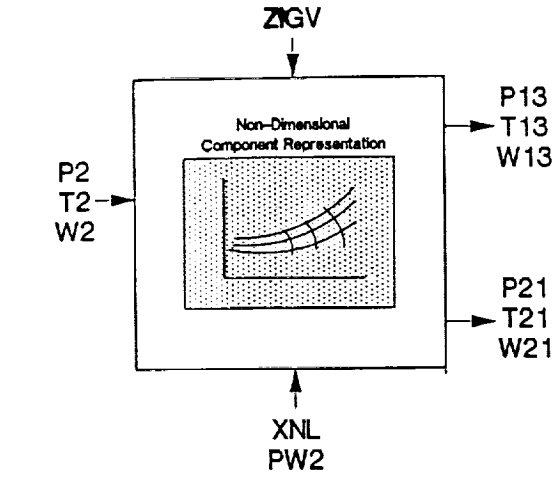

a) Generic fan block

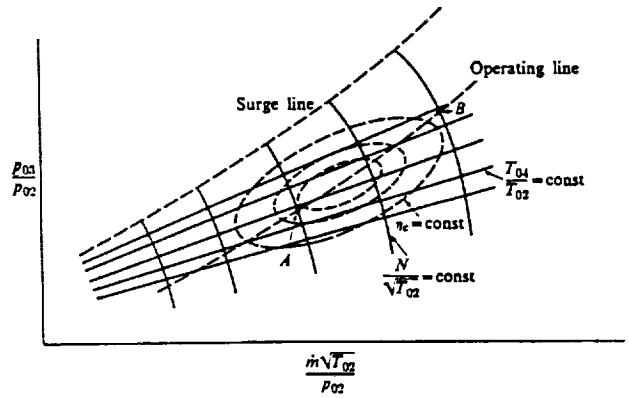

b) Conventional compressor map

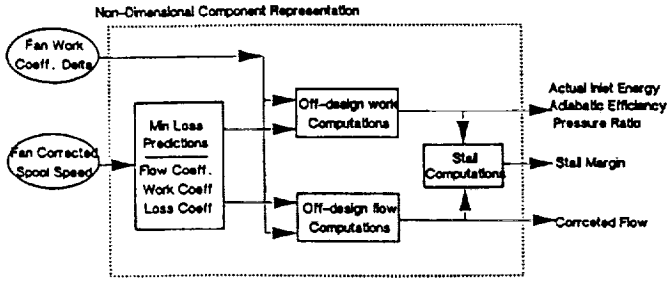

c) "Backbone" map

Fig. 7 Fan block approximations.

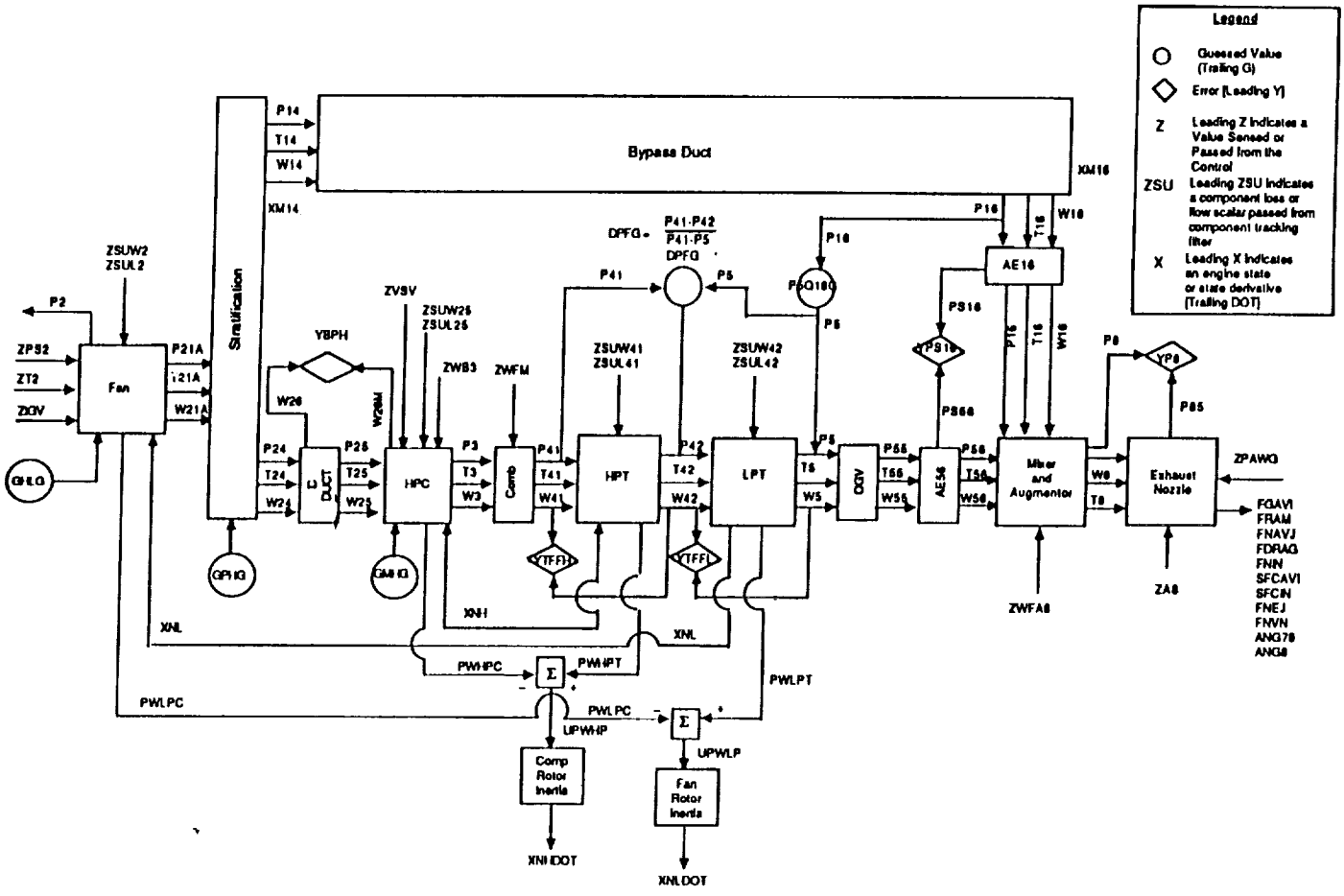

Fig. 8 Gas generator logic for a typical turbofan engine.

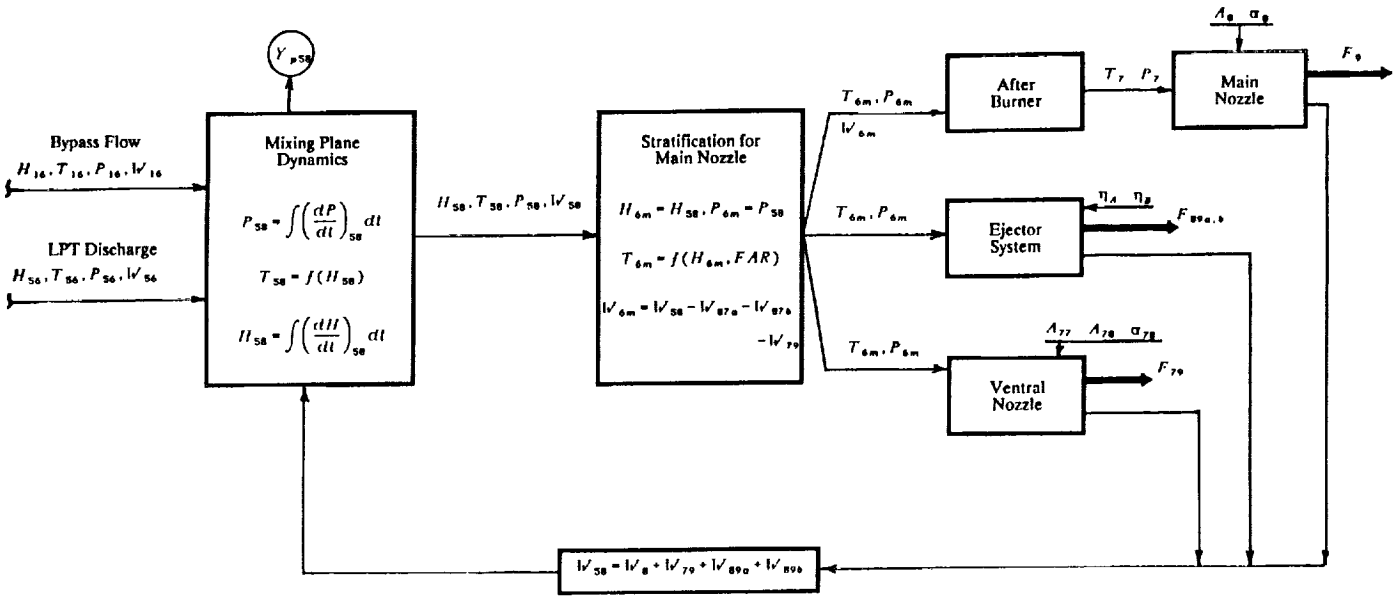

Fig. 9 Component level model of STOVL specific thrust effectors.

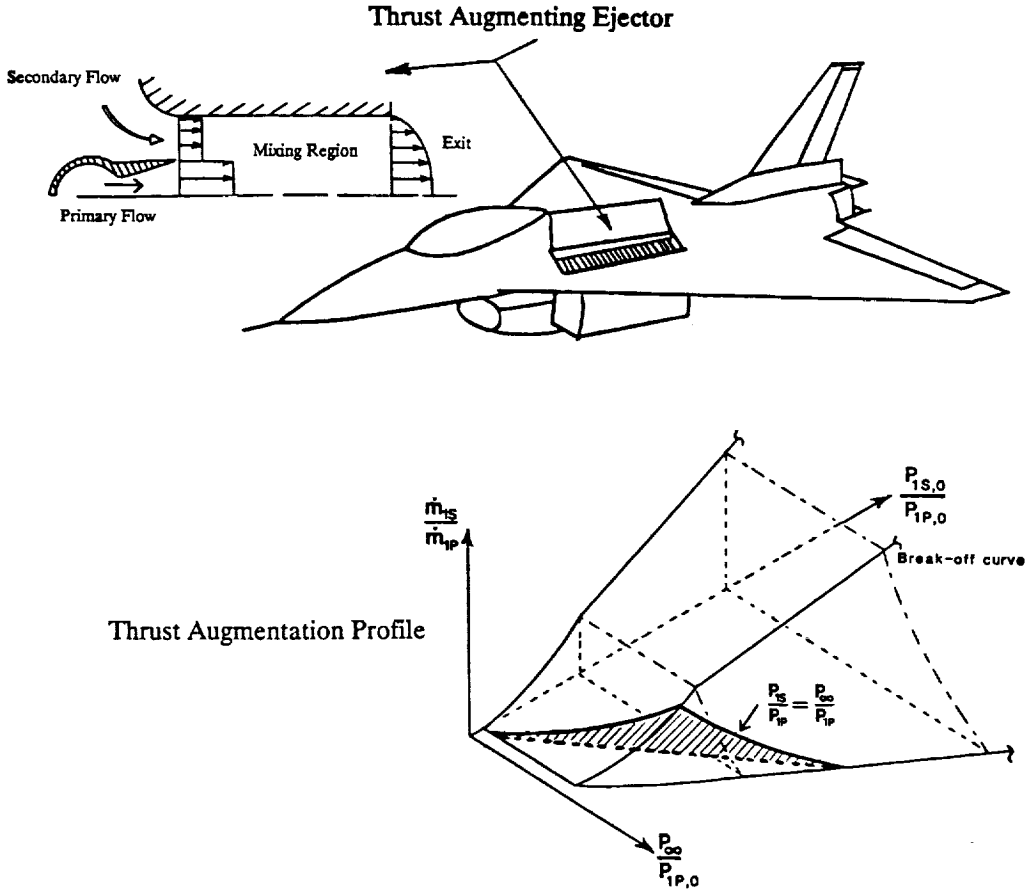

Fig. 10 Typical thrust augmenting ejector performance map.

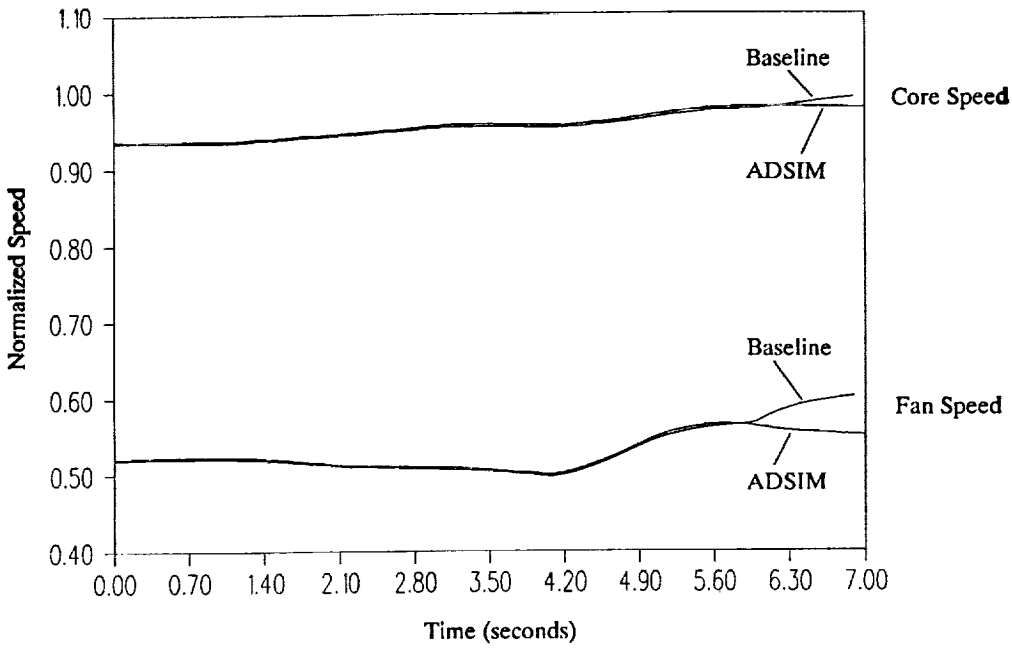

Fig. 11 Spool speed history for multiple effector operation

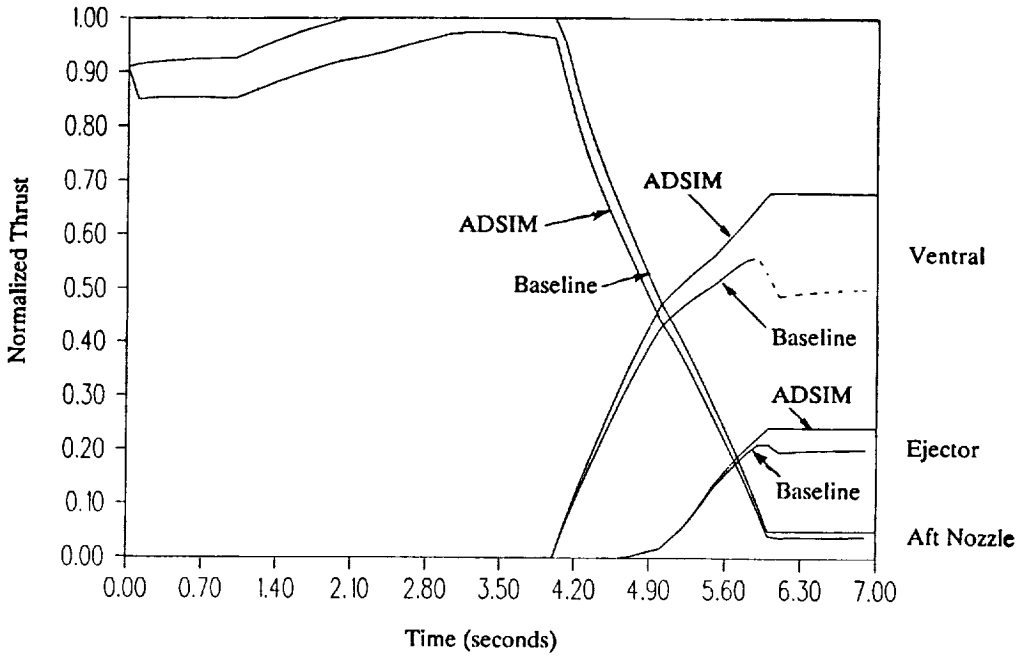

Fig. 12 Thrust history for multiple effector operation

NASA
National Aeronautics and Space Administration

Report Documentation Page

1. Report No.	2. Government Accession No.	3. Recipient's Catalog No.
NASA TM-102409		

4. Title and Subtitle	5. Report Date
Real-Time Simulation of an F110/STOVL Turbofan Engine	November 1989
	6. Performing Organization Code

7. Author(s)	8. Performing Organization Report No.
Colin K. Drummond and Peter J. Ouzts	E-5162
	10. Work Unit No.
	505-62-71

9. Performing Organization Name and Address	11. Contract or Grant No.
National Aeronautics and Space Administration Lewis Research Center Cleveland, Ohio 44135-3191	
	13. Type of Report and Period Covered
	Technical Memorandum

12. Sponsoring Agency Name and Address	14. Sponsoring Agency Code
National Aeronautics and Space Administration Washington, D.C. 20546-0001	

15. Supplementary Notes

Prepared for the Central/Northeastern ADIUS Conference sponsored by Applied Dynamics International, Cleveland, Ohio, October 16-17, 1989.

16. Abstract

A traditional F110-type turbofan engine model has been extended to include a ventral nozzle and two thrust-augmenting ejectors for Short Take-Off Vertical Landing (STOVL) aircraft applications. Development of the real-time F110/STOVL simulation required special attention to the modeling approach to component performance maps, the low pressure turbine exit mixing region, and the tailpipe dynamic approximation. Simulation validation derives by comparing output from the ADSIM simulation with the output for a validated F110/STOVL General Electric Aircraft Engines FORTRAN deck. General Electric substantiated basic engine component characteristics through factory testing and full scale ejector data.

17. Key Words (Suggested by Author(s))	18. Distribution Statement
Real-time simulation Turbofan engine	Unclassified – Unlimited Subject Category 07

19. Security Classif. (of this report)	20. Security Classif. (of this page)	21. No of pages	22. Price*
Unclassified	Unclassified	22	A03

*For sale by the National Technical Information Service, Springfield, Virginia 22161